

The official seal of the University of Delaware, rendered in a lighter blue tone. It is circular with a central shield containing an open book. The book's pages are inscribed with the Latin motto: 'GRAMM PHILOL RHE TOR ETHICA' on the left and 'METAPH MATHEM PHYSICA' on the right. The outer ring of the seal contains the text 'UNIVERSITY OF DELAWARE' at the top and '1743' at the bottom, flanked by two stars. The seal is partially obscured by the text and other elements on the slide.

ELEG404/604: Digital Imaging &
Photography

Gonzalo R. Arce

Department of Electrical and Computer Engineering
University of Delaware

Chapter VIII

X-Ray discovery

In 1895 Wilhelm Rontgen discovered the X-rays, while working with a cathode ray tube in his laboratory. One of his first experiments was a film of his wife's hand.



Shoe Fitting X-Ray Device

Shoe stores in the 1920s until the 1950s installed X-ray fluoroscope machines as a promotion device.

CERTIFICATE

SHOE-FITTING TEST DATA FOR _____

1. ANKLE ROLL GOOD FAIR POOR

2. WEIGHT DISTRIBUTION

3. X-RAY FITTING TEST



SCIENTIFIC SHOE FITTING AT ITS BEST

On Dr. Scholl's Fluoroscopic Shoe X-ray you can see the position of the bones in your feet right through the shoe. In addition to this checkup other methods of scientific shoe fitting will be employed here during this special demonstration.

Dr. Scholl's SHOE FITTING EXPERTS FROM THE CHICAGO FACTORY

will be in our store
Monday, February 15th

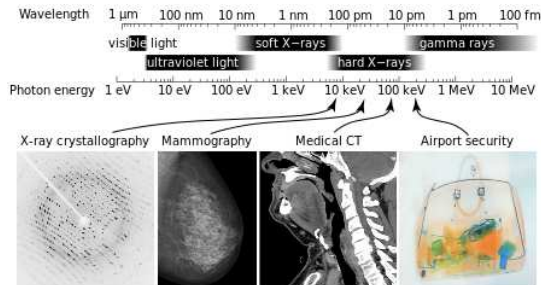
They bring with them the complete line of Dr. Scholl's Shoes (622 fittings) . . . every size, width and style — for every type foot. X-ray fitting—as well as other Dr. Scholl shoe fitting devices. Now you can obtain the shoe that will give you perfect satisfaction—and if you have foot troubles you will be shown how to obtain relief, quickly and inexpensively. Be sure to attend this great DISPLAY and DEMONSTRATION . . . first of its kind in this city.

GEO. S. MERCHANT
Winter Garden, Fla.

This scientific way of approaching the problem of poorly-fitted shoes eliminates guesswork. Now you can see for yourself!

Oak Ridge Associated Universities
Shoe-Fitting Fluoroscope (ca. 1930-1940)

X-Ray Spectrum

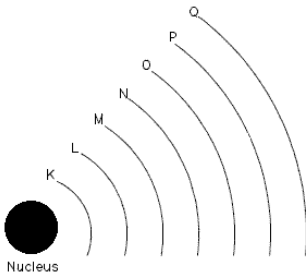


$$E = \hbar \cdot f = \hbar \frac{c}{\lambda}.$$

1 eV is the kinetic energy gained by an electron that is accelerated across a one volt potential.

- **Wavelength:** 0.01 - 10 nm.
- **Frequency:** 30 petahertz (3×10^{16}) to 30 exahertz (3×10^{19}).
- **Soft X-Rays:** 0.12 to 30 keV.
- **Hard X-Rays:** 30 to 120 keV.

Electron Binding Energy

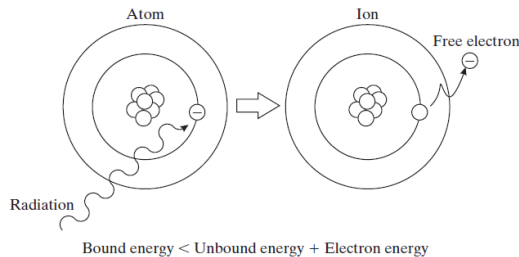


- When the ejection of one electron takes place, the energy of the resulting ion added with the energy of the free electron, is greater than the original energy of the atom. That is:

$$\textit{Bound energy} < \textit{Unbound energy} + \textit{Electron energy}$$

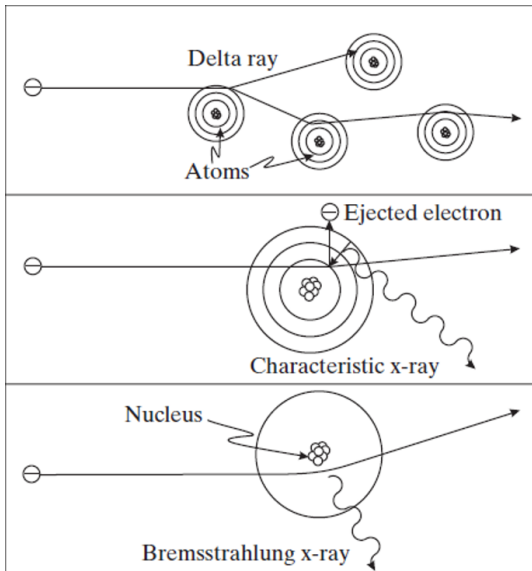
- The binding energy is the difference.
- It depends on the element to which the electron is bound.
- Average binding energy of lead 1 keV, tungsten 4 keV, hydrogen 13.6 eV.

Ionization and Excitation



- **Ionization:** Ejection of an electron from an atom, creating a free electron and an ion. The electron is ejected from the atom if the energy transferred by radiation to it, is equal or greater than the electron's binding energy.
- **Excitation:** Raising of an electron to a higher energy state e.g., an outer orbit.

Ionizing Radiation



Collisional Transfer

Incident electron collides with other electrons until it loses its kinetic energy.

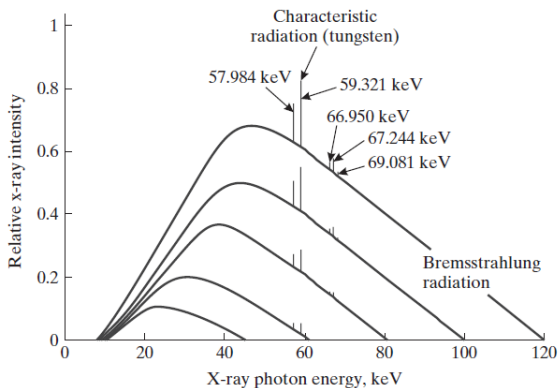
Characteristic Radiation

Incident electron ejects a K-shell electron generating a characteristic X-ray.

Bremsstrahlung Radiation

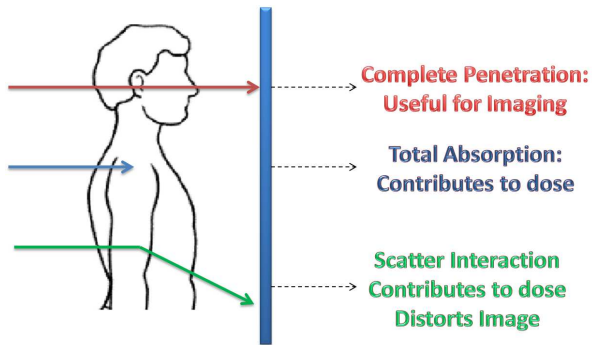
Incident electron is "broken" by a nucleus, generating "breaking" radiation

Spectrum of X-Ray



The different curves correspond to different potentials applied to the tube: 45kV, 61kV, 80kV, 100kV and 120 kV. The particular spectral lines correspond to characteristic radiation of Tungsten.

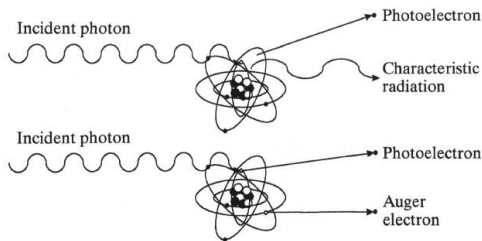
X-Ray interaction with matter



The main mechanisms by which Electromagnetic ionizing radiation interacts with matter are:

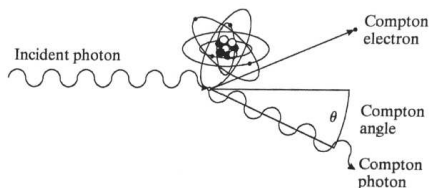
- Photoelectric effect
- Compton Scattering
- Pair Production

Photoelectric effect



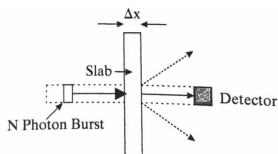
- The photon is not scattered, it is totally absorbed.
- This photon ejects an inner shell electron.
- The photoelectric effect is more likely to occur in absorbers of high atomic number (e.g. bone or positive contrast media)
- Contributes significantly to patient dose.
- Responsible for the contrast of the image.

Compton Scattering



- Photon collides with outer-shell electron, producing a new energetic electron called Compton electron.
- The incident photon, the Compton photon, changes its direction and loses energy as a result of the interaction.
- Undesirable for diagnostic radiography, and represents a source of radiation for the personnel conducting the diagnosis.
- It is as likely to occur with soft tissue as bone.

X-Ray Attenuation



- Photon fluence

$$\Phi = \frac{N}{A}$$

- Photon fluence rate

$$\phi = \frac{N}{A\Delta t}$$

- Energy fluence

$$\Psi = \frac{N\hbar\nu}{A}$$

- Energy fluence rate

$$\psi = \frac{N\hbar\nu}{A\Delta t}$$

- Energy fluence rate is also known as intensity

$$I = E\phi$$

- Considering the homogeneous slab of thickness Δx , and μ as the linear attenuation coefficient, the fundamental photon attenuation law is:

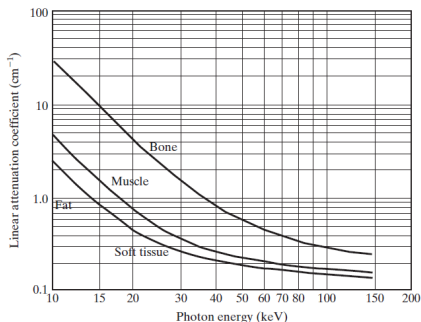
$$N = N_0 e^{-\mu\Delta x}$$

And in terms of intensity:

$$I = I_0 e^{-\mu\Delta x}$$

- N is the number of photons, A denotes area, t denotes time, $\hbar\nu$ is the energy of a photon. N_0 and I_0 are the number of photons at $x=0$ and the intensity of the incident beam respectively.

Linear attenuation coefficient



When the slab is non uniform, that is the linear attenuation coefficient varies along the slab, supposing the mono energetic case:

$$I(x) = I_0 e^{-\int_0^x \mu(x') dx'}$$

Where $I(x)$ is the x-ray intensity at position x .

Exposure

- Given by the symbol X
- Number of ion pairs produced in a specific volume of air by electromagnetic radiation.
- SI units: C/kg
- Common units: Roentgen, R
- $1\text{C/kg} = 3876\text{ R}$

Dose

- Given by the symbol D
- The general definition is:

$$D = \frac{\text{absorbed energy}}{\text{tissue mass}}$$

- SI units: Grays (Gy) J/kg
- Common units for dose: rad.
- 1 roentgen of exposure yields one rad of absorbed dose in soft tissue.

Dose Equivalent


- Different types of radiation, when delivering the same dose have different effects on the body.
- The symbol H is used

$$H = D \cdot Q$$



- Where Q is the quality factor, determined as a property of the radiation used.e.g. $Q \approx 1$ for x-rays, gamma rays, electrons; $Q \approx 10$ for neutrons and protons; $Q \approx 20$ for alpha particles.
- When D is measured in rads, H is considered to have units rems.
- When D is measured in grays, H is considered to have units sievert (Sv).

Radiation Dose in X-Ray and CT Exams



Doctors use "effective dose" when they talk about the risk of radiation to the entire body. Risk refers to possible side effects, such as the chance of developing a cancer later in life. Effective dose takes into account how sensitive different tissues are to radiation

	Procedure	Approximate effective radiation dose	Comparable to natural background radiation for:
ABDOMINAL REGION 	Computed Tomography (CT)–Abdomen and Pelvis	10 mSv	3 years
	Computed Tomography (CT)–Abdomen and Pelvis, repeated with and without contrast material	20 mSv	7 years
	Computed Tomography (CT)–Colonography	6 mSv	2 years
	Intravenous Pyelogram (IVP)	3 mSv	1 year
	Barium Enema (Lower GI X-ray)	8 mSv	3 years
	Upper GI Study with Barium	6 mSv	2 years

Radiation Dose in X-Ray and CT Exams

BONE	Procedure	Approximate effective radiation dose	Comparable to natural background radiation for:
	Spine X-ray	1.5 mSv	6 months
	Extremity (hand, foot, etc.) X-ray	0.001 mSv	3 hours
CENTRAL NERVOUS SYSTEM	Procedure	Approximate effective radiation dose	Comparable to natural background radiation for:
	Computed Tomography (CT)–Head	2 mSv	8 months
	Computed Tomography (CT)–Head, repeated with and without contrast material	4 mSv	16 months
	Computed Tomography (CT)–Spine	6 mSv	2 years

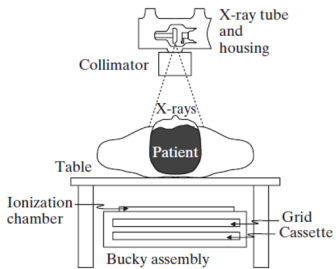
Radiation Dose in X-Ray and CT Exams

CHEST	Procedure	Approximate effective radiation dose	Comparable to natural background radiation for:
	Computed Tomography (CT)–Chest	7 mSv	2 years
	Computed Tomography (CT)–Lung Cancer Screening	1.5 mSv	6 months
	Chest X-ray	0.1 mSv	10 days
DENTAL	Procedure	Approximate effective radiation dose	Comparable to natural background radiation for:
	Dental X-ray	0.005 mSv	1 day

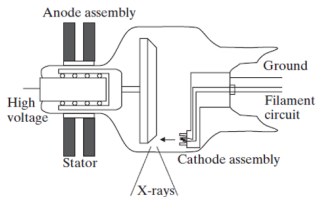
Biological Effects

- The main risk from ionizing radiation at the doses involved in medical imaging is cancer production.
- Injury to living tissue from the transfer of energy to atoms and molecules of the body.
- Can cause acute effects such as: skin reddening, hair loss and radiation burns.
- The general public should not be exposed to more than 100mrem/year.

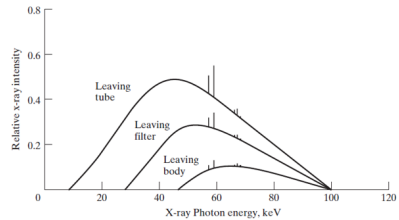
X-ray Tubes



Radiographic system

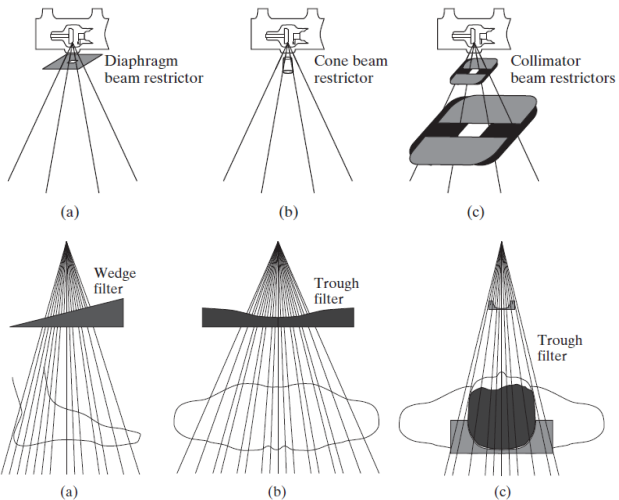


X-ray Tube Diagram

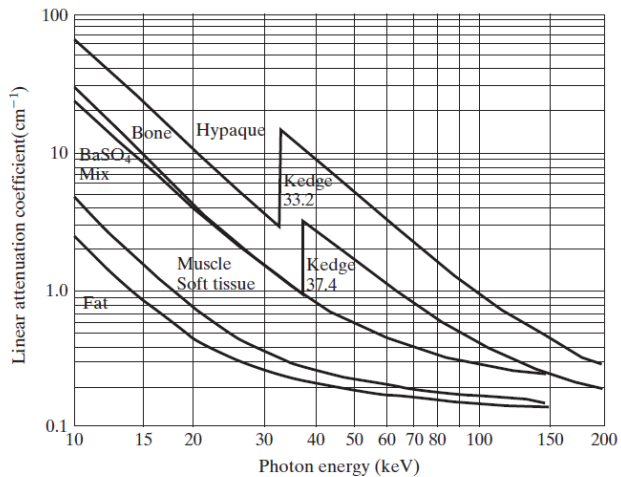


X-ray Spectra

Restriction Beam and Compensation Filters



Contrast Agents



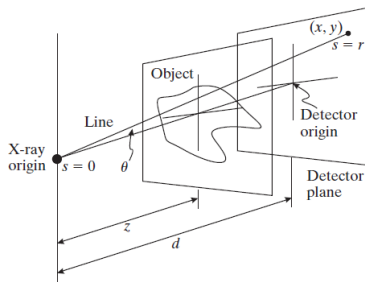
Imaging Equations

Monochromatic X-ray Source:

$$I(x, y) = I_0 e^{-\int_0^{r(x,y)} \mu(s; x, y) ds}$$

Polychromatic X-ray Source:

$$I(x, y) = \int_0^{E_{max}} \left\{ S_0(E') E' e^{-\int_0^{r(x,y)} \mu(s; E', x, y) ds}, dE' \right\} \quad (1)$$



Intensity

Taking into account the inverse square law, obliquity, the path length, the objects magnification, the usage of a non-uniform slab and the PSF of the film, the equation for intensity can be rewritten as:

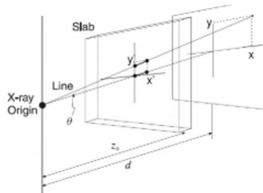
$$I_a(x, y) = I_0 \cos^3 \theta \cdot \left\{ \frac{1}{4\pi d^2 m^2} s \left(\frac{x}{m}, \frac{y}{m} \right) \right\} * t_z \left(\frac{x}{M}, \frac{y}{M} \right) * h(x, y)$$

Extended source
 $m =$ source magnification
 $s =$ source intensity distribution

PSF of film

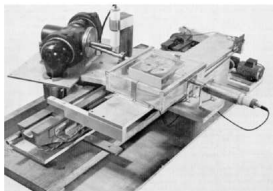
Inverse square + obliquity

Transmissivity of object



Reconstruction History

Hounsfield's experimental CT:

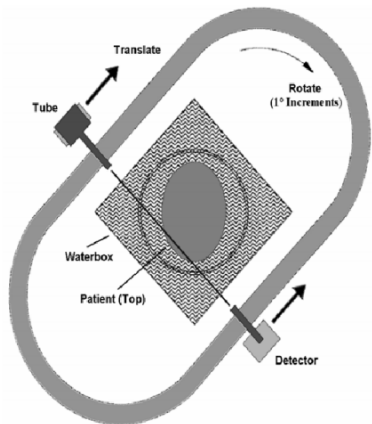


- Reconstruction methods based on Radon's work
 - 1917-classic image reconstruction from projections paper
- 1972 - Hounsfield develops the first commercial x-ray CT scanner

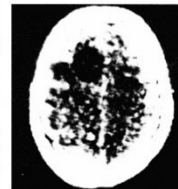
- Hounsfield and Cormack receive the 1979 Nobel Prize for their CT contributions
- Classical reconstruction is based on the Radon transform
 - Method known as backprojection
- Alternative approaches
 - Fourier Transform and iterative series-expansion methods
 - Statistical estimation methods
 - Wavelet and other multiresolution methods
 - Sub-Nyquist sampling: Compressed sensing and Partial Fourier Theories

1st Generation CT: Parallel Projections

Hounsfield's Experimental CT



- 1 Beam and 1 Detector
- 160 samples/traverse: 5min
- 1° increments over 180°
- 28,800 samples
- Solved simultaneous equations (Fortran): **2.5h**
- 160² image matrix but reduced to 80² for practical clinical use

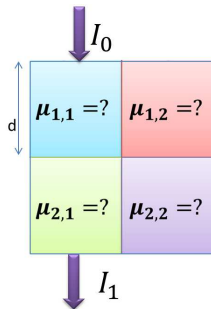


Example

$\mu_{1,1} = ?$	$\mu_{1,2} = ?$
$\mu_{2,1} = ?$	$\mu_{2,2} = ?$

Suppose an object that has 4 materials arranged in the boxes shown above. How can we find the linear attenuation coefficients?

Image Reconstruction



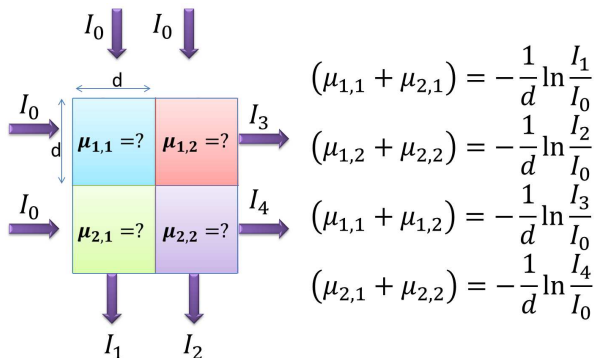
Suppose an x-ray of intensity I_0 is passing through the first column of the object, and that I_1 is the intensity measured at the other side.

$$I_1 = I_0 e^{-(\mu_{1,1} + \mu_{2,1})d}$$

$$\ln \frac{I_1}{I_0} = -(\mu_{1,1} + \mu_{2,1})d$$

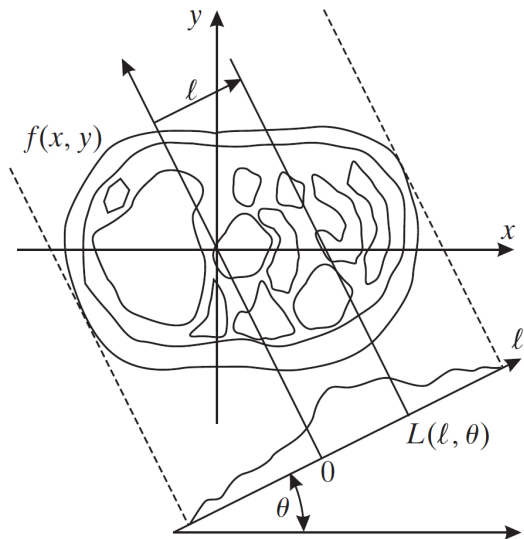
$$(\mu_{1,1} + \mu_{2,1}) = -\frac{1}{d} \ln \frac{I_1}{I_0}$$

Image Reconstruction



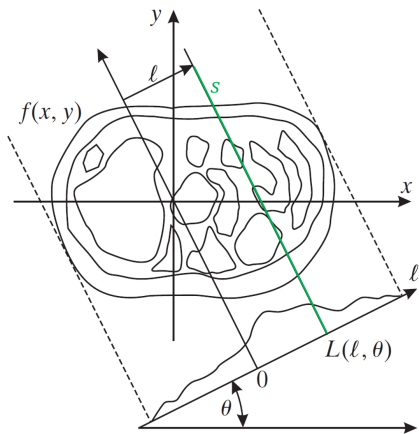
If we repeat the same process for each of the rows and the columns, we obtain the equations necessary to obtain the values of the coefficients. However for bigger systems, the number of equations is not practical for implementation.

Radon Transform



- $f(x, y)$ describes our object
- How to describe $f(x, y)$ in terms of its projections onto a line c
- Let l be the distance along the line $L(l, \theta)$ starting from the origin.

Radon Transform



- For a fixed projection angle θ , and a particular linear shift of the X-ray beam, a projection integral is given by:

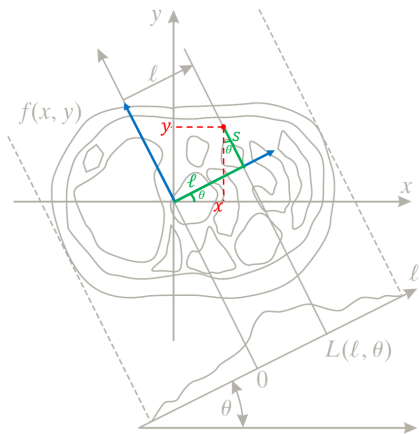
$$g(l, \theta) = \int_{-\infty}^{\infty} f(x(s), y(s)) ds$$

- **Example:** If $\theta = 0$

$$g(l, \theta = 0) = \int_{-\infty}^{\infty} f(l, y) dy$$

- **Example:** If $\theta = 90$

$$g(l, \theta = 90) = \int_{-\infty}^{\infty} f(x, l) dx$$

Radon Transform $\forall \theta$ 

Option 1

Rotate the coordinate system so that l and the projection direction (axis of integration) are horizontal and vertical

$$x(s) = l \cos \theta - s \sin \theta$$

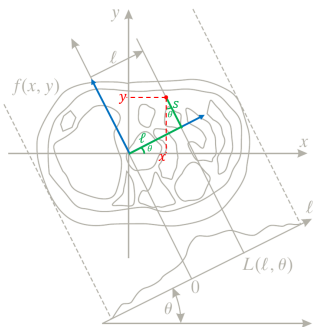
$$y(s) = l \sin \theta + s \cos \theta$$

$$g(l, \theta) = \int_{-\infty}^{\infty} f(x(s), y(s)) ds$$

Radon Transform $\forall \theta$

Option 2

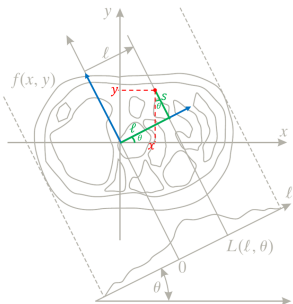
Instead of rotating the object and integrating, integrate the object only along the line $L(\ell, \theta)$



$$g(\ell, \theta) = \int_{-\infty}^{\infty} \int_{-\infty}^{\infty} f(x, y) \delta(x \cos \theta + y \sin \theta - \ell) dx dy$$

- The sifting property causes the integrand to be zero everywhere except on $L(\ell, \theta)$

How does the Radon Transform apply to X-rays



Recall that $I_d = I_0 \exp\left(-\int_0^d \mu(x(s), y(s)) ds\right)$ is the received X-ray intensity of a beam projected through an object along the line s . Taking logarithms at both sides:

$$-\ln\left(\frac{I_d}{I_0}\right) = \int_0^d \mu(x(s), y(s)) ds$$

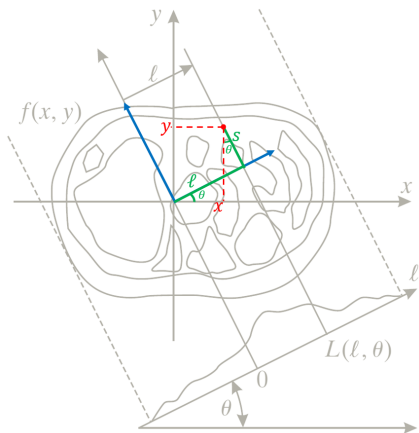
Then the Radon transform describes the X-ray projections for $g(\ell, \theta) = -\ln\left(\frac{I_d}{I_0}\right)$ and $f(x, y) = \mu(x, y)$.

$$x(s) = \ell \cos \theta - s \sin \theta$$

$$y(s) = \ell \sin \theta + s \cos \theta$$

$$g(\ell, \theta) = \int_{-\infty}^{\infty} f(x(s), y(s)) ds$$

How does the Radon Transform apply to X-rays



Radon Transform

In CT we measure $g(\ell, \theta) = -\ln\left(\frac{I_d}{I_0}\right)$ and need to find $f(x, y) = \mu(x, y)$ using

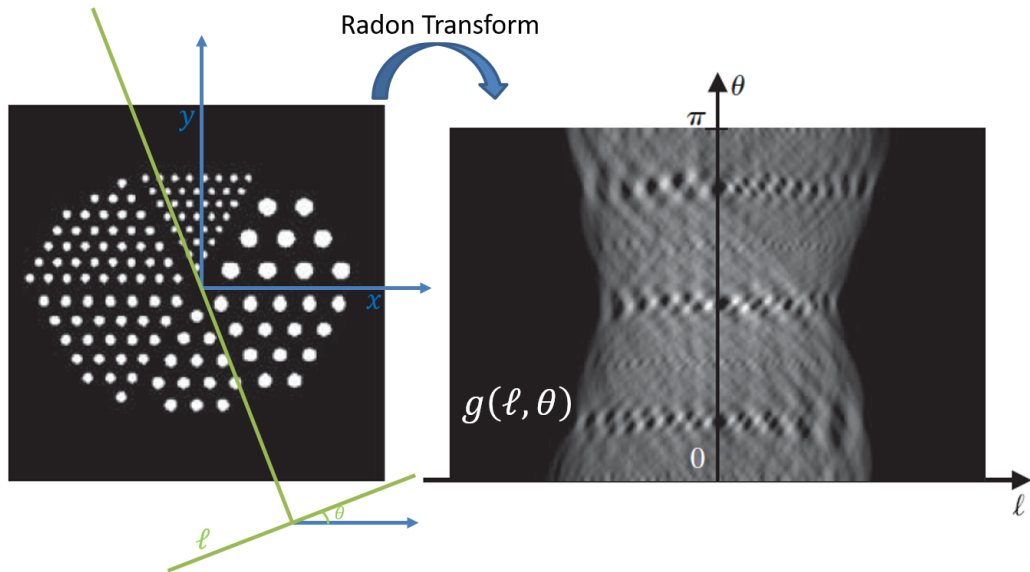
$$g(\ell, \theta) = \int_{-\infty}^{\infty} f(x(s), y(s)) ds$$

$$x(s) = \ell \cos \theta - s \sin \theta$$

$$y(s) = \ell \sin \theta + s \cos \theta$$

Sinogram

A sinogram is an image of $g(\ell, \theta)$



Backprojection Method

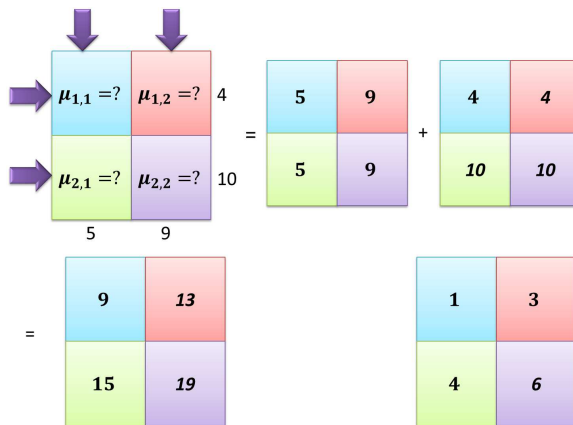
Intuition: If $g(\ell, \theta_0)$ takes on a large value at $\ell = \ell_0$, then $f(x, y)$ must be large over the line (or somewhere on the line) $L(\ell_0, \theta_0)$.



One way to create an image with this property is to assign every point on $L(\ell_0, \theta_0)$ the value $g(\ell_0, \theta_0)$, i.e. $b_\theta = g(x \cos \theta + y \sin \theta, \theta)$.

Back Projection Example

With the example of the 4 boxes given before, we back project the results obtained. As it can be seen, the right answer is not obtained, however the order of the numbers is the same:

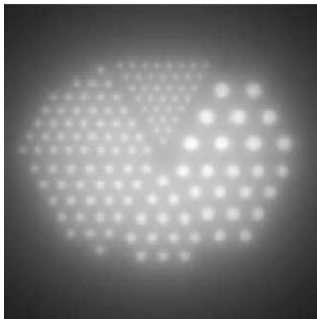


Problems with Backprojection Method

- Bright spots tend to reinforce, which results in a blurry image.
- Problem:

$$f_b(x, y) = \int_0^\pi b_\theta(x, y) d\theta \neq f(x, y)$$

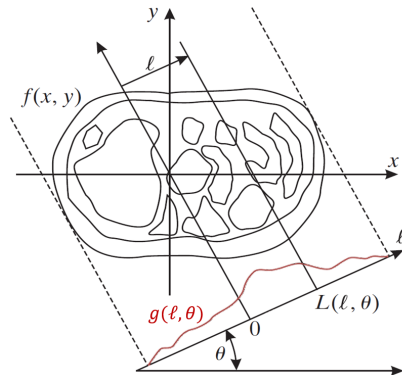
- Resulting Image (Laminogram):



Projection-Slice Theorem

Take the 1D Fourier transform of a projection $g(\ell, \theta)$

$$G(\rho, \theta) = \mathcal{F}_{1D} \{g(\ell, \theta)\} = \int_{-\infty}^{\infty} g(\ell, \theta) e^{-j2\pi\rho\ell} d\ell$$



Projection Slice Theorem

From the 1D Fourier Transform of a projection $g(\ell, \theta)$

$$G(\rho, \theta) = \mathcal{F}_{1D} \{g(\ell, \theta)\} = \int_{-\infty}^{\infty} g(\ell, \theta) e^{-j2\pi\rho\ell} d\ell$$

Next we substitute the Radon transform for $g(\ell, \theta)$

$$g(\ell, \theta) = \int_{-\infty}^{\infty} \int_{-\infty}^{\infty} f(x, y) \delta(x \cos \theta + y \sin \theta - \ell) dx dy$$

$$G(\rho, \theta) = \int_{-\infty}^{\infty} \int_{-\infty}^{\infty} \int_{-\infty}^{\infty} f(x, y) \delta(x \cos \theta + y \sin \theta - \ell) e^{-j2\pi\rho\ell} dx dy d\ell$$

Rearranging

$$G(\rho, \theta) = \int_{-\infty}^{\infty} \int_{-\infty}^{\infty} f(x, y) \left\{ \int_{-\infty}^{\infty} \delta(x \cos \theta + y \sin \theta - \ell) e^{-j2\pi\rho\ell} d\ell \right\} dx dy$$

Projection-Slice Theorem

What does this look like?

$$G(\rho, \theta) = \int_{-\infty}^{\infty} \int_{-\infty}^{\infty} f(x, y) \left\{ e^{-j2\pi\rho[x \cos\theta + y \sin\theta]} \right\} dx dy$$

$$G(\rho, \theta) = \int_{-\infty}^{\infty} \int_{-\infty}^{\infty} f(x, y) \left\{ e^{-j2\pi[x\rho \cos\theta + y\rho \sin\theta]} \right\} dx dy$$

It is reminiscent of the 2D Fourier transform of $f(x, y)$, defined as

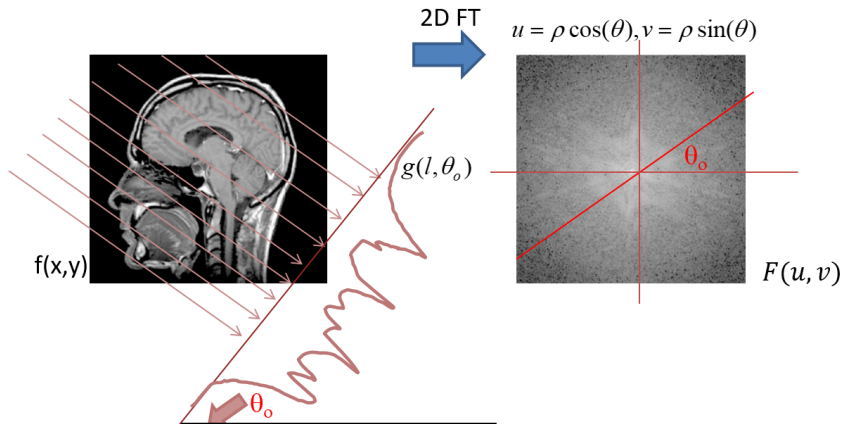
$$F(u, v) = \int_{-\infty}^{\infty} \int_{-\infty}^{\infty} f(x, y) e^{-j2\pi(xu + yv)} dx dy$$

Let $u = \rho \cos\theta$ and $v = \rho \sin\theta$, then

$$G(\rho, \theta) = F(\rho \cos\theta, \rho \sin\theta)$$

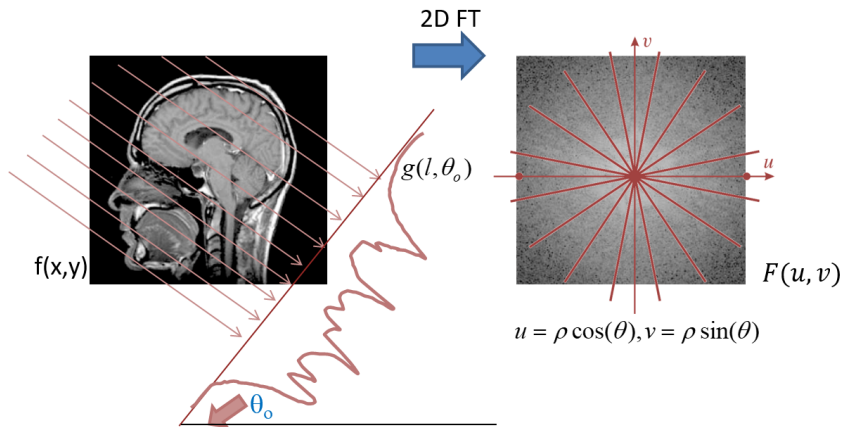
Projection-Slice Theorem

The 1-D Fourier transform of a projection is a *slice* of the 2D Fourier transform of the object



Fourier Reconstruction Method

Take projections at all angles θ . Take the 1D FT to build $F(u, v)$ one slice at a time. Take the Inverse 2D-FT of the result.



Fourier Reconstruction Method

- The projection slice theorem leads to the following reconstruction method:
 - Take 1D Fourier Transform of each projection to obtain $G(\rho, \theta)$ for all θ .
 - Convert $G(\rho, \theta)$ to Cartesian grid $F(u, v)$.
 - Take inverse 2D Fourier Transform to obtain $f(x, y)$.
- It is not used because it is difficult to interpolate polar data into a Cartesian grid, and the inverse 2D Fourier Transform is time consuming

Filtered Back Projection

Consider the inverse Fourier Transform in 2D: In polar coordinates ,
 $u = \rho \cos \theta$ and $v = \rho \sin \theta$, the inverse Fourier transform can be written as

$$f(x, y) = \int_0^{2\pi} \int_0^{\infty} F(\rho \cos \theta, \rho \sin \theta) e^{j2\pi\rho[x \cos \theta + y \sin \theta]} \rho d\rho d\theta$$

Using the projection-slice theorem $G(\rho, \theta) = F(\rho \cos \theta, \rho \sin \theta)$, we have

$$f(x, y) = \int_0^{2\pi} \int_0^{\infty} G(\rho, \theta) e^{j2\pi\rho[x \cos \theta + y \sin \theta]} \rho d\rho d\theta$$

Since $g(\ell, \theta) = g(-\ell, \theta + \pi)$ it follows that

$$f(x, y) = \int_0^\pi \int_{-\infty}^{\infty} |\rho| G(\rho, \theta) e^{j2\pi\rho[x \cos\theta + y \sin\theta]} d\rho d\theta.$$

Furthermore, from the integration over ρ , the term $x \cos\theta + y \sin\theta$ is a constant, say ℓ . Hence,

$$f(x, y) = \int_0^\pi \left[\int_{-\infty}^{\infty} |\rho| G(\rho, \theta) e^{j2\pi\rho\ell} d\rho \right] d\theta$$

- Filter Response.
 - $c(\rho) = |\rho|$.
 - High pass filter.
- $G(\rho, \theta)$ is more densely sampled when ρ is small.
- The ramp filter compensate for the sparser sampling at higher ρ .

Convolution Back Projection

From the filtered back projection algorithm we get

$$f(x, y) = \int_0^\pi \left[\int_{-\infty}^{\infty} |\rho| G(\rho, \theta) e^{j2\pi\rho\ell} d\rho \right] d\theta$$

From the convolution theorem of the FT, we can rewrite $f(x, y)$ as

$$f(x, y) = \int_0^\pi \left[\mathcal{F}_{1D}^{-1} \{|\rho|\} * g(\ell, \theta) \right] d\theta.$$

Defining $c(\ell) = \mathcal{F}_{1D}^{-1} \{|\rho|\}$,

$$\begin{aligned} f(x, y) &= \int_0^\pi [c(\ell) * g(\ell, \theta)] d\theta \\ &= \int_0^\pi \int_{-\infty}^{\infty} g(\ell, \theta) c(x \cos \theta + y \sin \theta - \ell) d\ell d\theta \end{aligned}$$

Problem: $c(\ell)$ does not exist, since $|\rho|$ is not integrable.

Convolution Back Projection

Practical Solution: Windowing ρ

Define

$$\tilde{c}(\ell) = \mathcal{F}_{1D}^{-1} \{ |\rho| W(\rho) \},$$

where $W(\rho)$ is a windowing function that filters the observed projection in addition to the ramp filter.

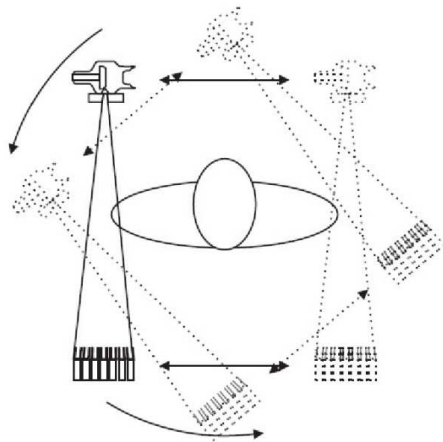
$$f(x, y) = \int_0^\pi [\tilde{c}(\ell) * g(\ell, \theta)] d\theta$$

Common windows

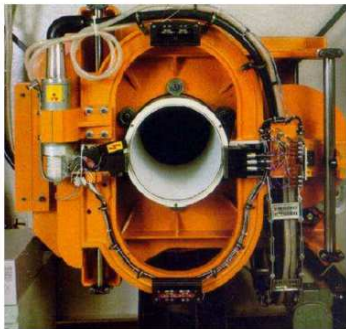
- Hamming window
- Lanczos window (Sinc function)
- Simple rectangular window
- Ram-Lak window
- Kaiser window
- Shepp-Logan window

2nd Generation

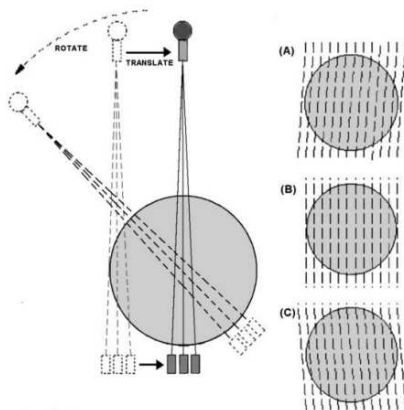
- Incorporated linear array of 30 detectors
- More data acquired to improve image quality
- Shortest scan time was 18 seconds/slice
- Narrow fan beam allows more scattered radiation to be detected



2nd Generation

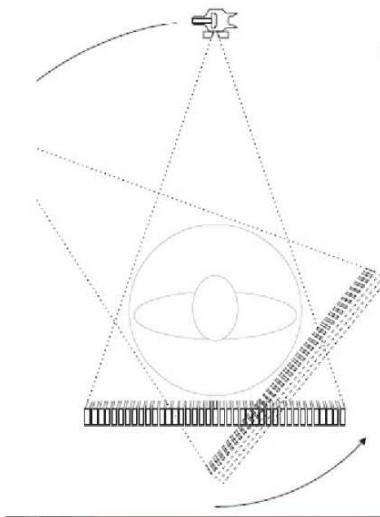


- Multiple detectors
- Still translate-rotate
 - 1 view acquired per detector ($\sim 1^\circ$ apart)
 - angular increment increased by using more detectors



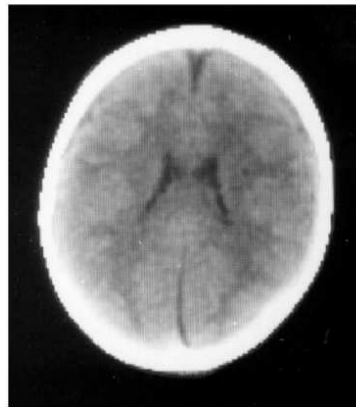
3rd Generation

- Number of detectors increased substantially (more than 800 detectors)
- Angle of fan beam increased to cover entire patient (no need for translational motion)
- Mechanically joined x-ray tube and detector array rotate together
- Newer systems have scan times of 1/2 second



2nd and 3rd Generation Reconstructions**1972: 5 Minutes** **1976: 2 Seconds**

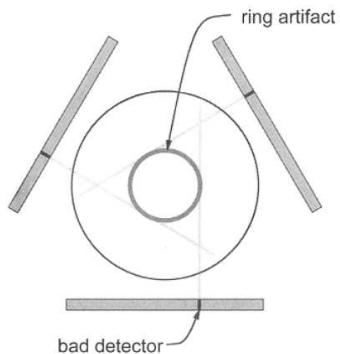
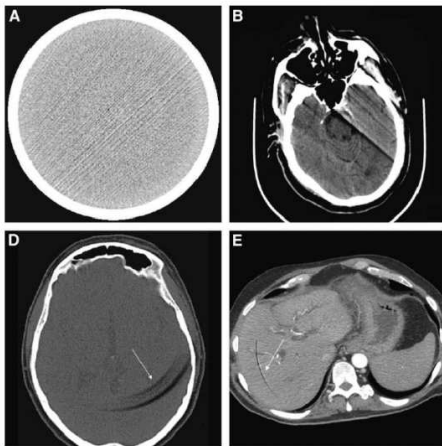
2G



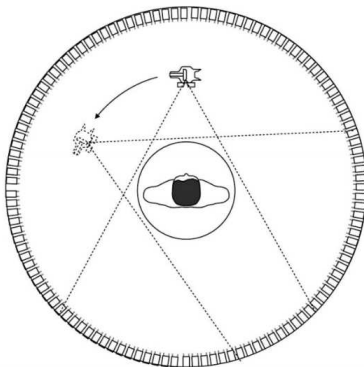
3G

3rd Generation Artifacts

Ring Artifacts

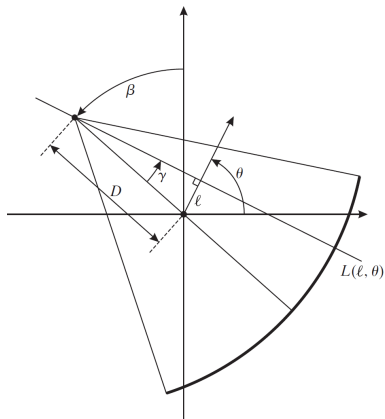


4th Generation



Designed to overcome the problem of artifacts. Stationary ring of about 4800 detectors

Fan Beam Reconstruction



- Fan-beam parameters

$$\theta = \beta + \gamma$$

$$l = D \sin \gamma,$$

- D is the distance from source to the origin (isocenter)
- Recall the parallel-ray CBP

$$f(x, y) = \int_0^\pi \int_{-\infty}^{\infty} g(l, \theta) c(x \cos \theta + y \sin \theta - l) dl d\theta$$

- Assuming $g(l, \theta) = 0$ for $|l| > T$.

$$f(x, y) = \frac{1}{2} \int_0^{2\pi} \int_{-T}^T g(l, \theta) c(x \cos \theta + y \sin \theta - l) dl d\theta$$

Fan Beam Reconstruction

- Let (r, ϕ) be the polar coordinates of a point (x, y) . Then $x = r \cos \phi$, $y = r \sin \phi$ and $x \cos \theta + y \sin \theta = r \cos \theta \cos \phi + r \sin \phi \sin \theta = r \cos(\theta - \phi)$. Then:

$$f(r, \phi) = \frac{1}{2} \int_0^{2\pi} \int_{-T}^T g(\ell, \theta) c(r \cos(\theta - \phi) - \ell) d\ell d\theta$$

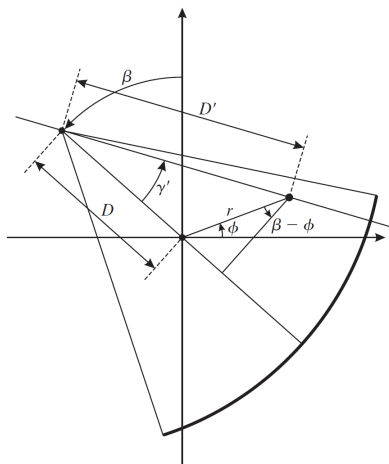
- Using the Jacobian of the transformation: $\theta = \beta + \gamma$ and $\ell = D \sin \gamma$.

$$f(r, \phi) = \frac{1}{2} \int_{-\gamma}^{2\pi - \gamma} \int_{\sin^{-1} \frac{-T}{D}}^{\sin^{-1} \frac{T}{D}} g(D \sin \gamma, \beta + \gamma) c(r \cos(\beta + \gamma - \phi) - D \sin \gamma) D \cos \gamma d\gamma d\beta$$

- The expression $\sin^{-1} \frac{T}{D}$ represents the largest angle that needs to be considered given an object of radius T , γ_m . Furthermore, functions are periodic in β with period 2π , then:

$$f(r, \phi) = \frac{1}{2} \int_0^{2\pi} \int_{-\gamma_m}^{\gamma_m} p(\gamma, \beta) c(r \cos(\beta + \gamma - \phi) - D \sin \gamma) D \cos \gamma d\gamma d\beta$$

Fan Beam Reconstruction



- The argument of $c(\cdot)$ can be written in simpler form using these coordinates

$$r \cos(\beta + \gamma - \phi) - D \sin \gamma = D' \sin(\gamma' - \gamma)$$

- Then, the reconstruction can be rewritten as

$$f(r, \phi) = \frac{1}{2} \int_0^{2\pi} \int_{-\gamma_m}^{\gamma_m} p(\gamma, \beta) c(D' \sin(\gamma' - \gamma)) D \cos \gamma d\gamma d\beta$$

- Recall $c(\ell) = \int_{-\infty}^{\infty} |\rho| e^{j2\pi\rho\ell} d\rho$. Then:

$$c(D' \sin(\gamma)) = \int_{-\infty}^{\infty} |\rho| e^{j2\pi\rho D' \sin(\gamma)} d\rho$$

Fan-Beam Reconstruction

If we substitute $\rho' = \frac{\rho D' \sin(\gamma)}{\gamma}$, in $c(D' \sin(\gamma)) = \int_{-\infty}^{\infty} |\rho| e^{j2\pi\rho D' \sin(\gamma)} d\rho$. It can be shown that

$$c(D' \sin(\gamma)) = \left(\frac{\gamma}{D' \sin(\gamma)} \right)^2 c(\gamma').$$

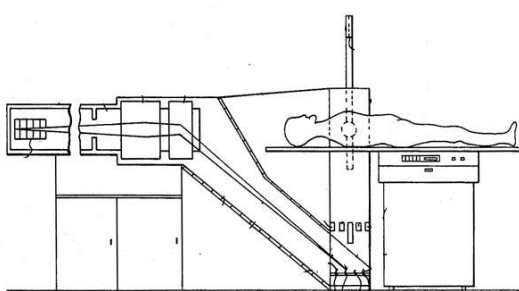
Let $c_f = \frac{1}{2} D \left(\frac{\gamma}{\sin(\gamma)} \right)^2 c(\gamma)$, then

$$f(r, \phi) = \int_0^{2\pi} \int_{-\gamma_m}^{\gamma_m} \tilde{p}(\gamma, \beta) c_f(\gamma' - \gamma) d\gamma d\beta,$$

where $\tilde{p}(\gamma, \beta) = \cos(\gamma)p(\gamma, \beta)$

5G: Electron Beam CT (EBCT)

- Developed specifically for cardiac tomographic imaging.
- No conventional x-ray tube; large arc of tungsten encircles patient and lies directly opposite to the detector ring
- Electron beam steered around the patient to strike the annular tungsten target.



6G and 7G CT

6G: Electron Beam CT (EBCT)

- Helical CT scanners acquire data while the table moves, there is a single detector array.
- Allows the use of less contrast agent.

7G: Multislice

- CT becomes a cone beam
- 40 parallel detector rows
- 32mm detector length
- 16 0.5mm slices for second